

熱帯積雲対流に及ぼす大気大規模循環の効果

熱帯降雨観測衛星および気候モデルデータ 解析研究から

東京大学大気海洋研究所
高菺 縁

協力： 廣田渚郎、重尚一、W.-K. Tao
渡部雅弘、木本昌秀

09/19/2012神戸大セミナー

Effects of the large-scale circulation on tropical cumulus convection

Yukari N. Takayabu
Atmosphere Ocean Research Institute (AORI)
the Univ. Tokyo

Collaborators:

Nagio Hirota (U. Tokyo)
Shoichi Shige (Kyoto Univ)
Wei-Kuo Tao (NASA/GSFC)
Masahiro Watanabe (U. Tokyo)
Masahide Kimoto (U. Tokyo)

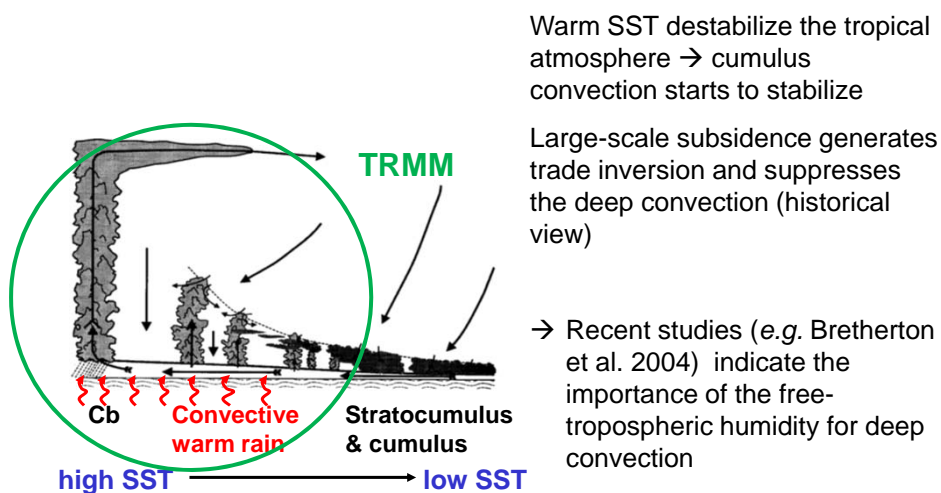
09/19/2012神戸大セミナー

目次

- 自由対流圏の湿度依存性に関する観測研究からの示唆
- TRMM衛星観測に見られる熱帯降雨の2レジーム: deepとshallow(ここではcongestus)
- CMIP3, CMIP5 気候モデルにおける対流パラメタリゼーションの湿度依存性
 - double ITCZ問題との関連
- CRM研究からの示唆

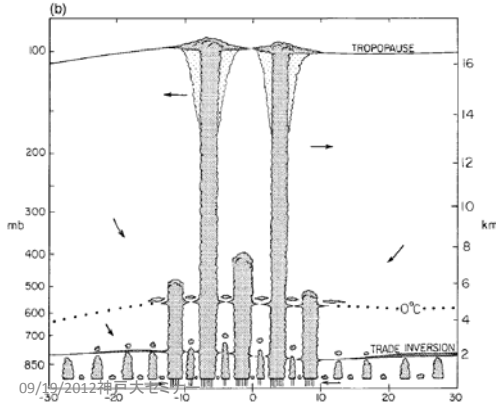
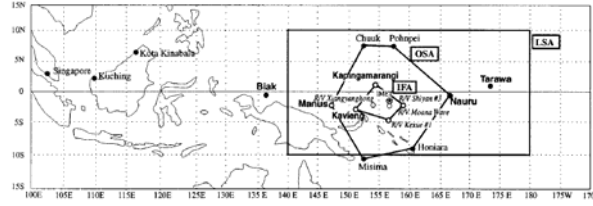
09/19/2012神戸大セミナー

Tropical clouds are under the influences of SST and large-scale circulation



09/19/2012神戸大セミナー

TOGA-COARE revealed the tri-modality of the tropical convection

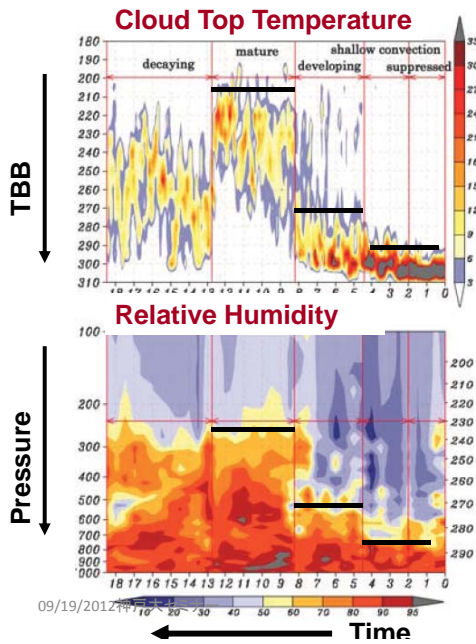


Abundance of cumulus congestus

Johnson et al. 1999

Effects of subsidence observed with the MJO

in TOGA-COARE period



Three-steps-wise development of convections is observed in association with MJO.

In the shallow-convection stage, mid-troposphere is very dry, indicating strong subsidence as a part of the MJO structure.

Kikuchi and Takayabu (2004, GRL)

Similarity of lifecycles in various organized convection systems

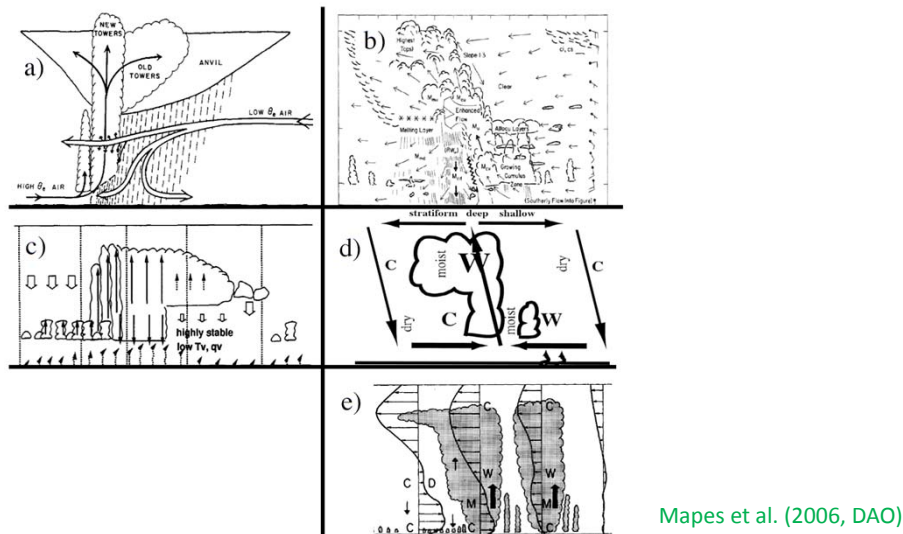
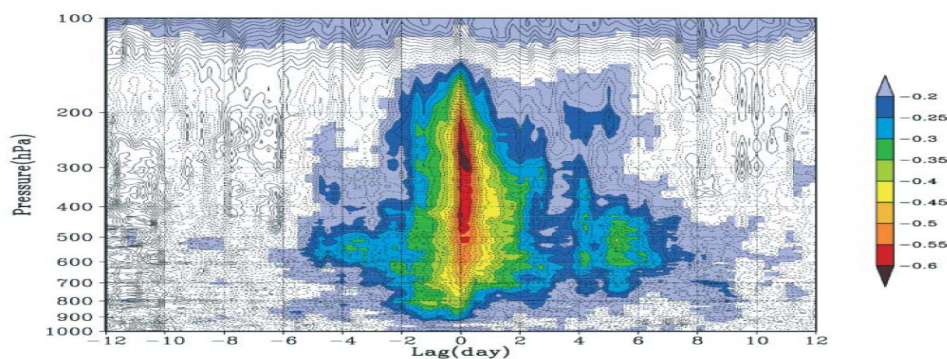


Fig. 1. Conceptual models of: a, b) mesoscale convective systems (Zipser 1969, Zipser et al.

1981); c) a two-day wave (Takayabu et al. 1996); d) a convectively coupled Kelvin wave (Straub and Kiladis 2003); and e) the Madden-Julian oscillation (Lin and Johnson 1996).

Lag-correlations btwn WV mixing ratio and GMS IR TBB

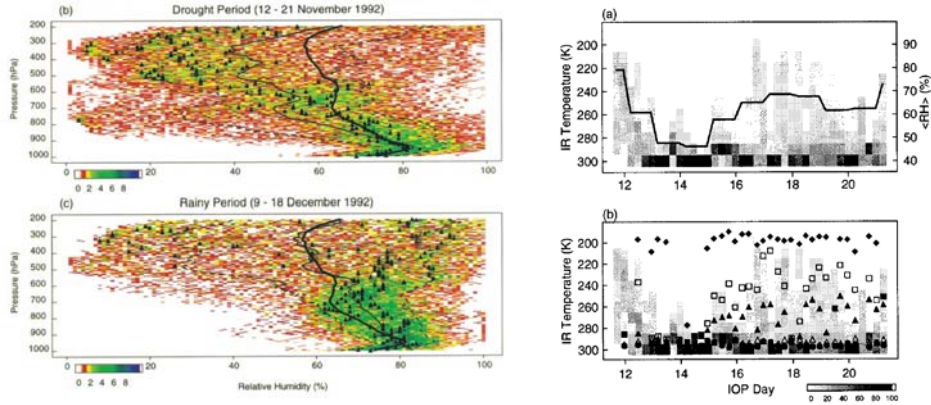
865 sondes launched over ocean from R/V Mirai, R/V Kaiyo, and R/V Natsushima



Takayabu, Yokomori et al. (2006, JMSJ)

Significance of mid-level humidity as a precursor of deep convection is suggested, consistent with Brown and Zhang (1997), Sherwood (1999), Bretherton et al. (2004), etc.

Brown and Zhang (1997)



Numaguti et al. (1995) and Yoneyama et al. (1995) suggested the mid-level dry intrusion associated with an MJO significantly suppressed the deep convection.

Consistently, in the drought period (Nov.12-21) of TOGA-COARE IOP, significant difference in RH is found in the mid-to-upper troposphere above 700hPa. (Brown and Zhang, 1997)

Bretherton et al. 2004

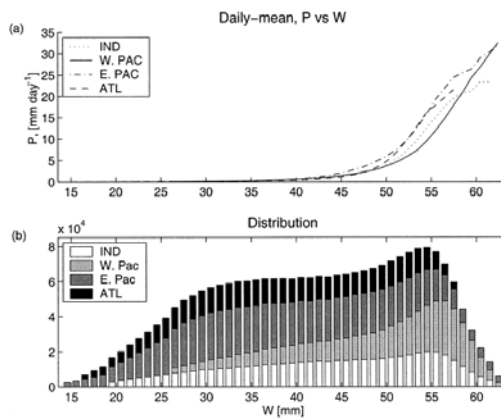


FIG. 2. (a) Mean daily averaged precipitation P in 1-mm-wide bins of water vapor path W , for the four tropical ocean regions in Fig. 1 for all months in 1998–2001. (b) Number of observations in each bin in the four regions.

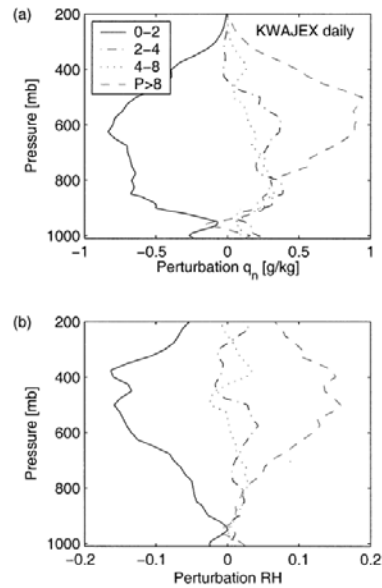
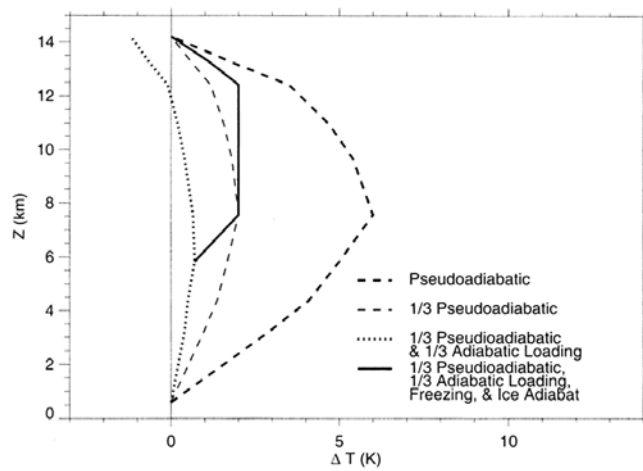


FIG. 10. Daily mean KWAJEX radiosonde-derived perturbation (a) normalized specific humidity and (b) relative humidity profiles binned averaged by daily mean radar-derived precipitation rate (mm day⁻¹).

Re-boost effect on the effective buoyancy with latent heating of freezing (Zipser, 2003)



- Discreteness of tropical convection
- Rareness of undiluted convection

09/19/2012神戸大セミナー

Takayabu, Y. N., S. Shige, W.-K. Tao, and N. Hirota, 2010, *J. Clim.*

SHALLOW AND DEEP LATENT HEATING MODES OVER TROPICAL OCEANS OBSERVED WITH TRMM PR SLH DATA

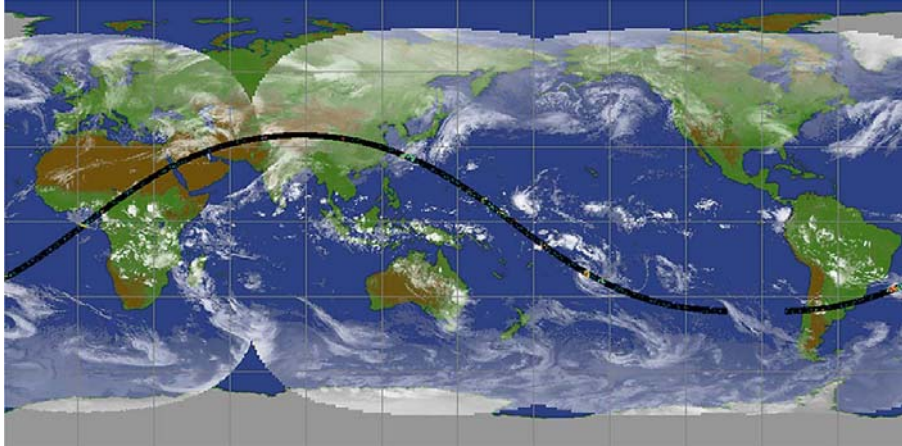
09/19/2012神戸大セミナー

Tropical Rainfall Measuring Mission

TRMM PR Single Orbit Rain Observation

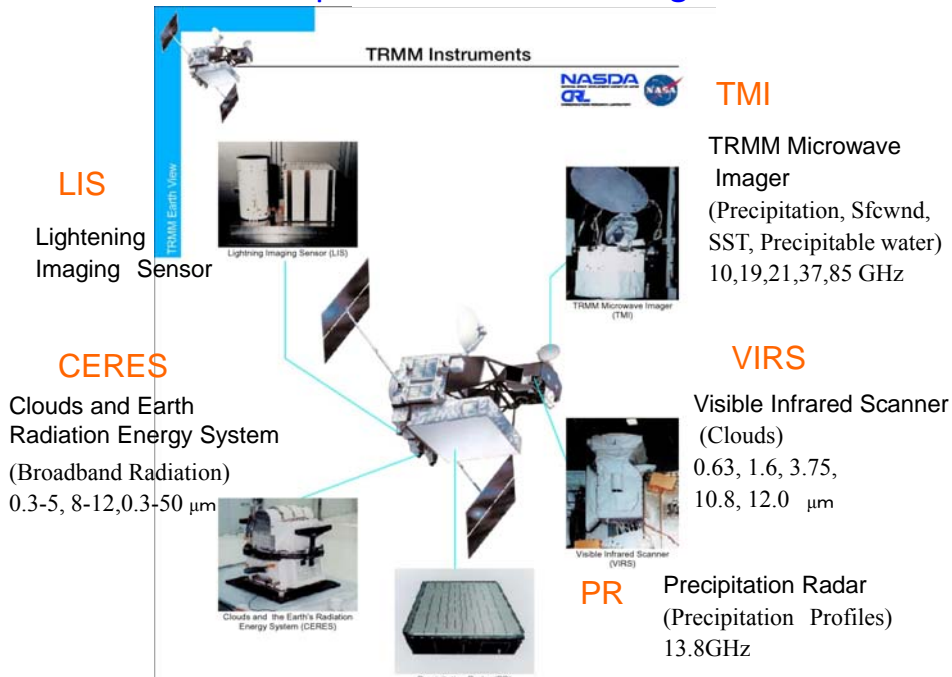
8 Dec 1997 16:41-18:13

presented by NASDA (JAXA)

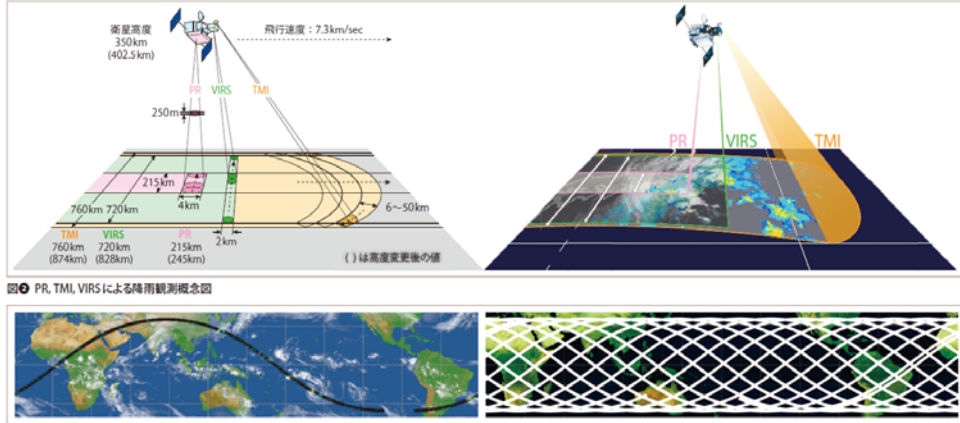


Swath width: ~220km Orbits: ~16 times/day

TRMM: Tropical Rainfall Measuring Mission

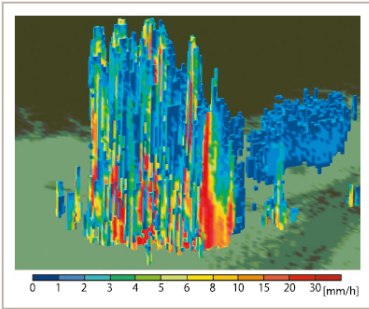
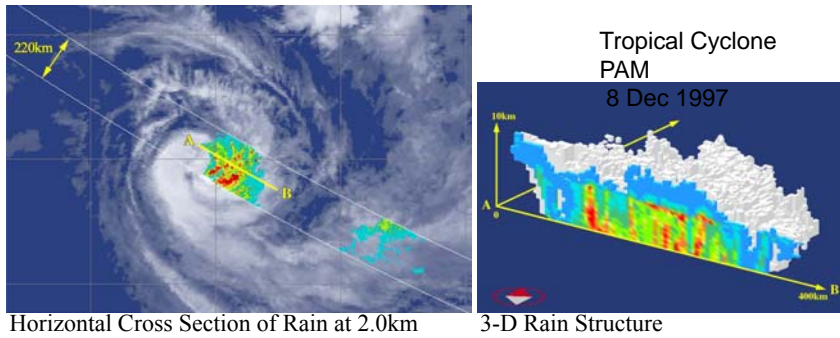


TRMM降雨観測



PR Swath width: 215km (245km) Orbits: ~16 times/day

TRMM PRによる3次元降雨観測



図③ 1998年5月28日20時59分(世界時)にTRMMで観測した降雨
バングラデシュ付近で観測された南側からのPRの立体画像と鉛直断面図

JAXA EORC 提供

降雨の日変化

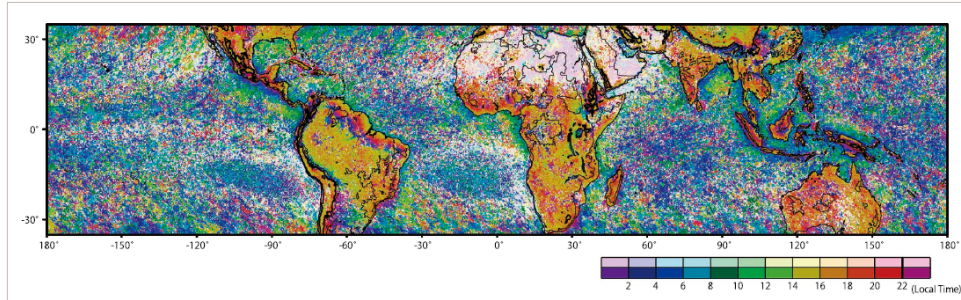


図9 TRMM マイクロ波放射計(TMI)による降水の日周変化
色は降雨量のもっとも多い地方時を示す。陸上で午後の雨(暖色系)、海上で午前の雨(寒色系)が多いことがわかる。

降雨特性: 降雨量/発雷比

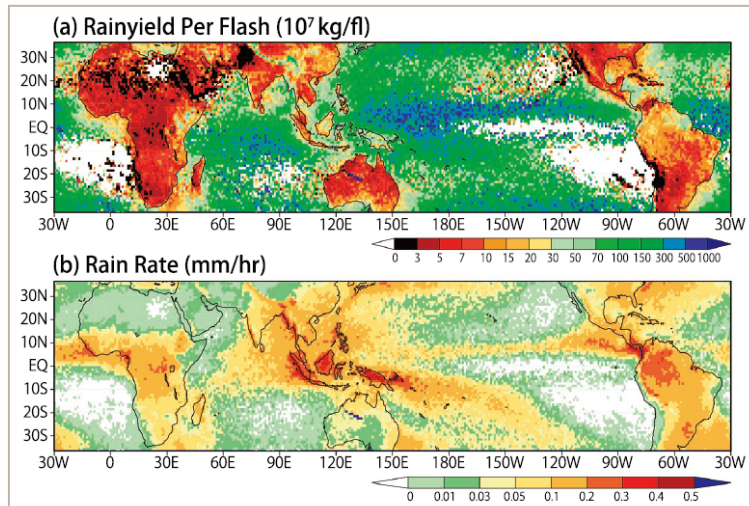


図10 TRMMのPRおよびLIS観測から求められた(a)3年平均の降雨/発雷比(RPF, 単位 10^7 kg/f)、および(b)8年平均降雨率全球分布(北緯 36° - 南緯 36°)

赤系の色は雷の多い性質の雨、青系は少ない雨を示す。海陸の降雨特性の違いが顕著である。

Takayabu, 2006

Apparent Heat Source (Yanai et al. 1973)

$$Q1 \equiv \frac{D\bar{s}}{Dt} = \frac{\partial \bar{s}}{\partial t} + \bar{v} \cdot \nabla \bar{s} + \bar{\omega} \frac{\partial \bar{s}}{\partial p}$$

$$= QR + L(\bar{c} - \bar{e}) - \nabla \cdot \overline{s'v'} - \frac{\partial}{\partial p} \overline{s'\omega'}$$

where $s = CpT + gz$ dry static energy

$\bar{\quad}$: grid mean, $'$: deviation from the grid mean

- 3D Q1-QR data from the SLH database are used:
generated in TRMM2A25 original resolution and gridded
into monthly, 0.5deg0.5deg: L3LH, Dec.1997-Nov.2007

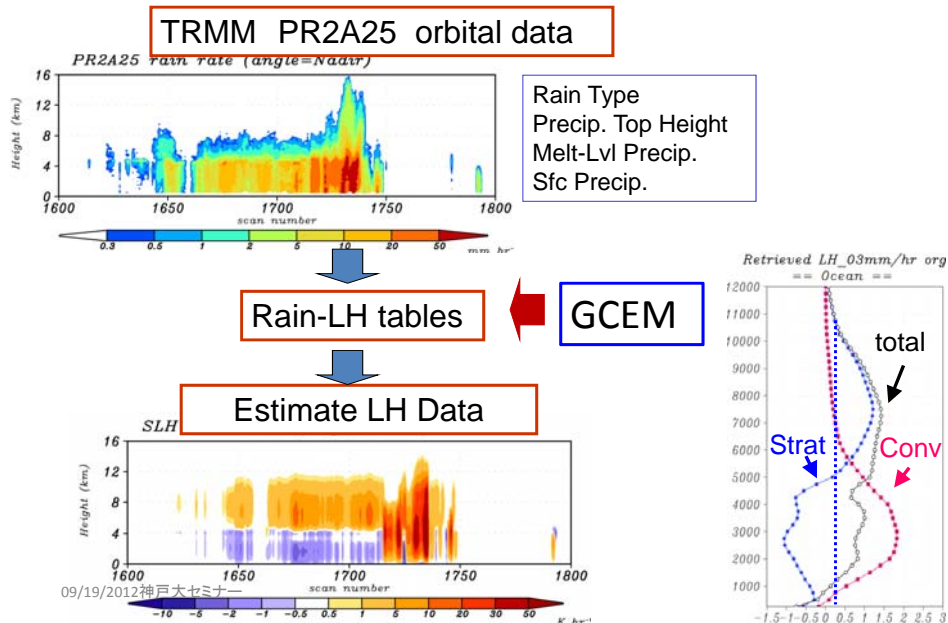
09/19/2012神戸大セミナー

Shige et al. (2004)

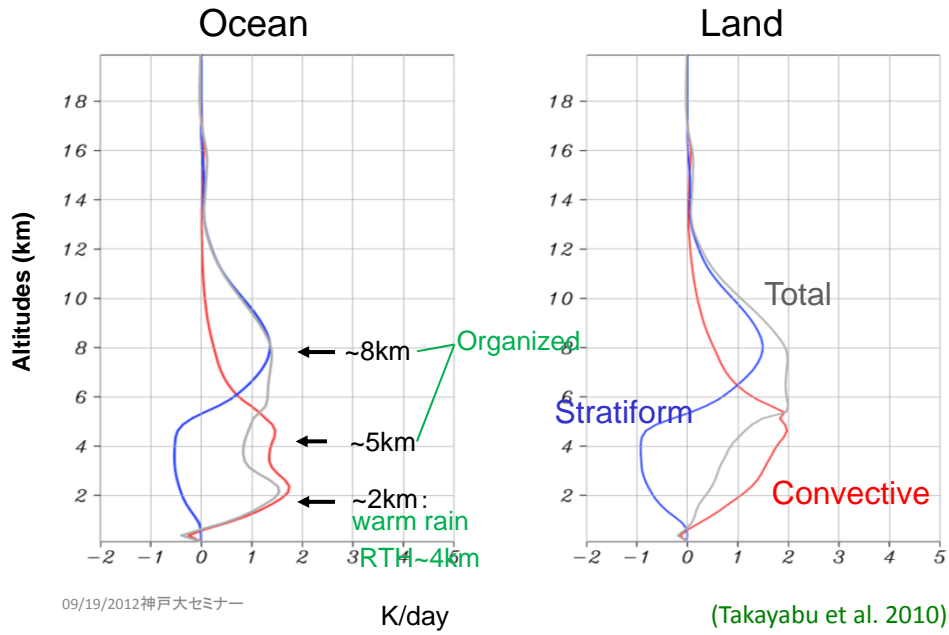
<http://www.eorc.jaxa.jp/TRMM/lh/index.html>

Data: TRMM Spectral Latent Heating (SLH)

Shige et al. 2004, JAMC



TRMM SLH Q1-QR ALL 98-07 20N-20S



09/19/2012神戸大セミナー

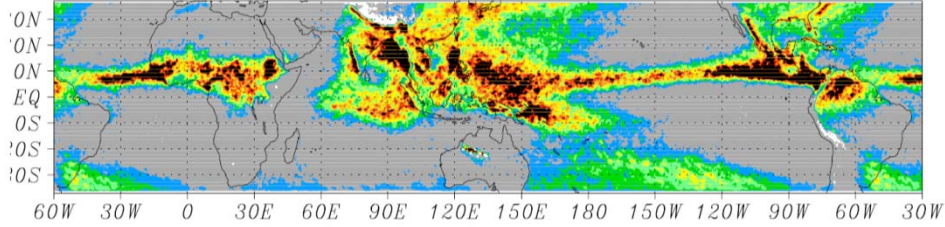


09/19/2012神戸大セミナー

10-year mean Q1-QR JJA 98-07

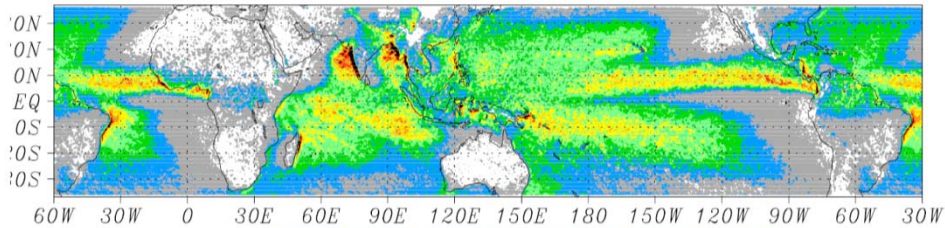
Deep Organized Systems

7.5km



Cumulus Congestus

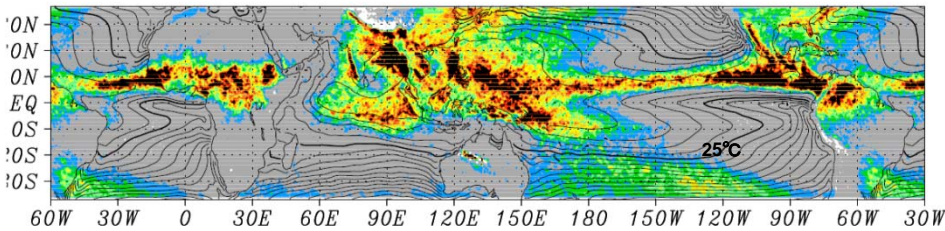
2.0km



10-year mean Q1-QR & SST JJA 98-07

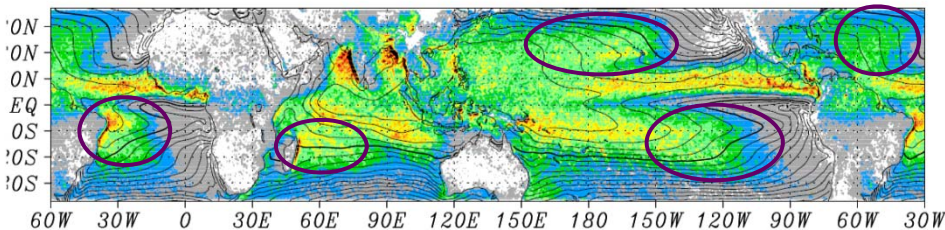
Deep Organized Systems

7.5km



Cumulus Congestus

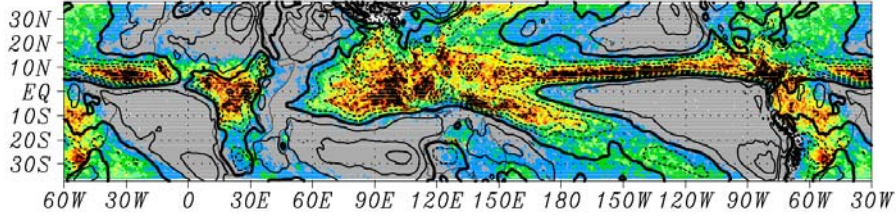
2.0km



10-year mean Q1-QR & ω_{500} JJA 98-07

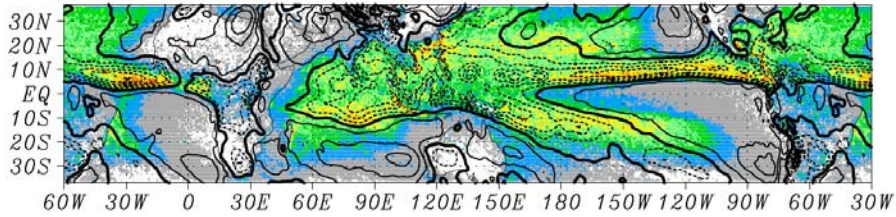
Deep Organized Systems

7.5km



Cumulus Congestus

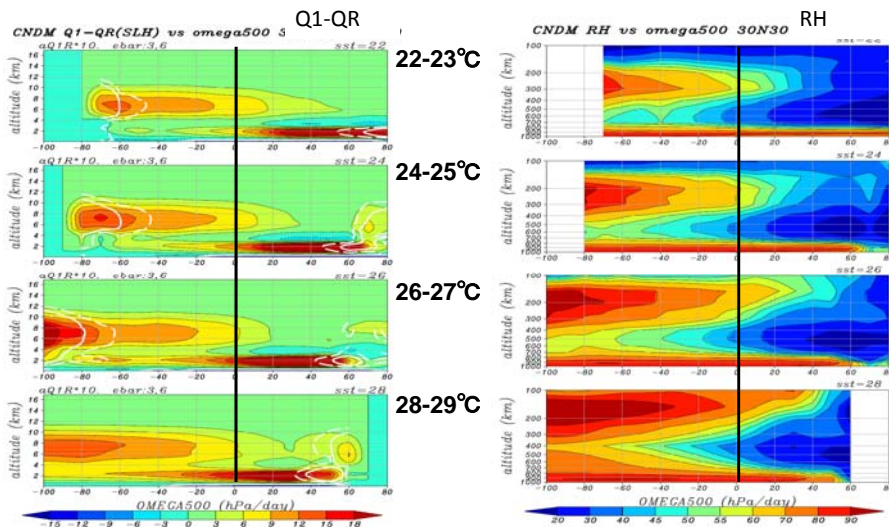
2.0km



09/19/2012神戸大セミナー

(Takayabu et al. 2010)

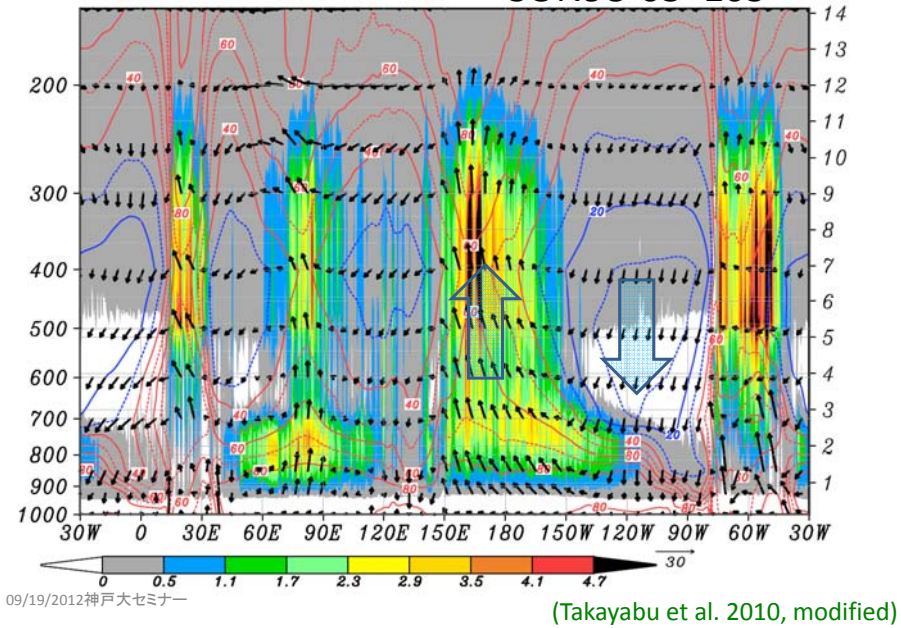
Cond-Mean Q1-QR & RH vs ω_{500} hPa 30N30S 9804



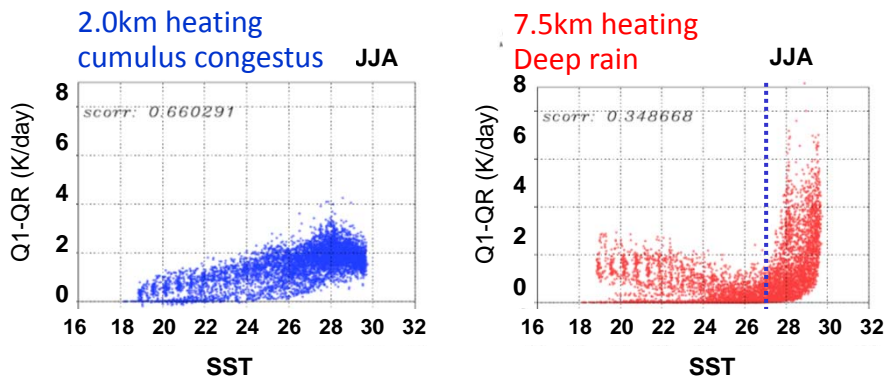
In order to separate the effects of large-scale circulation from those of SST, plots are separated in terms of SST. It was shown that similar significant dryness in the mid-to-lower troposphere is found in the subsidence region irrespective of the SST.

09/19/2012神戸大セミナー

TRMM SLH Q1-QR, JRA25 winds, RH SON98-05 10S



Unconditional mean Q1-QR vs. SST 97-05 30N-30S



While congestus responds linearly to SST, which means obedient to the low-level instability, deep rain is controlled by another factor.

From the TRMM SLH Analysis

- Distinct two regimes of convective heating with TRMM-PR based Q1-QR; a cumulus congestus rain with a peak at ~2km, and with a peak for deep organized rain at ~8km.
- Under large-scale subsidence, cumulus congestus rain dominates over ocean, but not over land.
- Congestus rain responds linearly to SST, while deep organized convection is effectively suppressed by large-scale subsidence, probably through the entrainment of free tropospheric dry air.

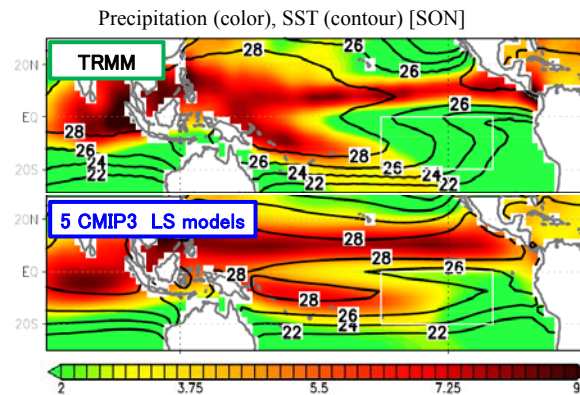
09/19/2012神戸大セミナー

Hirota, N., Y. N. Takayabu, M. Watanabe, and M. Kimoto, 2011
J. Climate

PRECIPITATION REPRODUCIBILITY OVER TROPICAL OCEANS AND ITS RELATIONSHIP TO THE DOUBLE ITCZ PROBLEM IN CMIP3 AND MIROC5* CLIMATE MODELS

*MIROC5: U.TOKYO/JAMSTEC/NIES NEW MODEL FOR CMIP5
09/19/2012神戸大セミナー

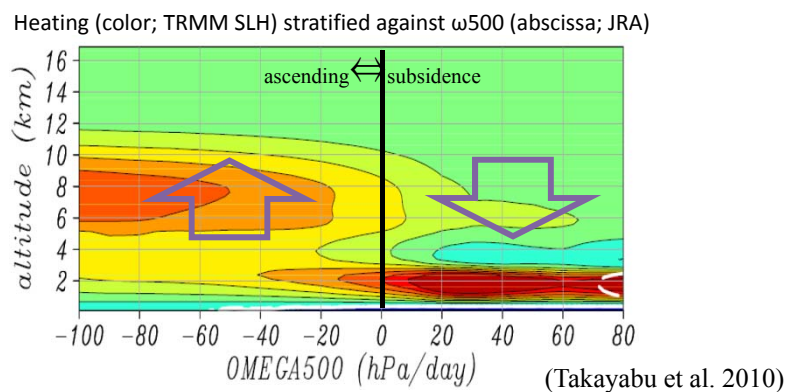
Double ITCZ in climate models



- Systematic precipitation bias over the southeastern Pacific (Mechoso et al. 1995; Szoeke and Xie 2008)
- Double ITCZ appears even in AGCMs (Zhang et al. 2007; Chikira, 2010)
- Mitigated by modification of convective parameterization (Song and Zhang 2009, Chikira 2010) (Hirota et al., 2011)

09/19/2012神戸大セミナー

Effects of SST and subsidence



- We have seen subsidence regions had very dry layer in the middle trop. (~600 hPa)
- Entrainment of dry air reduces buoyancy of convection
 - suppression of deep convection

09/19/2012神戸大セミナー

DOUBLE ITCZ IN CMIP3 MODELS

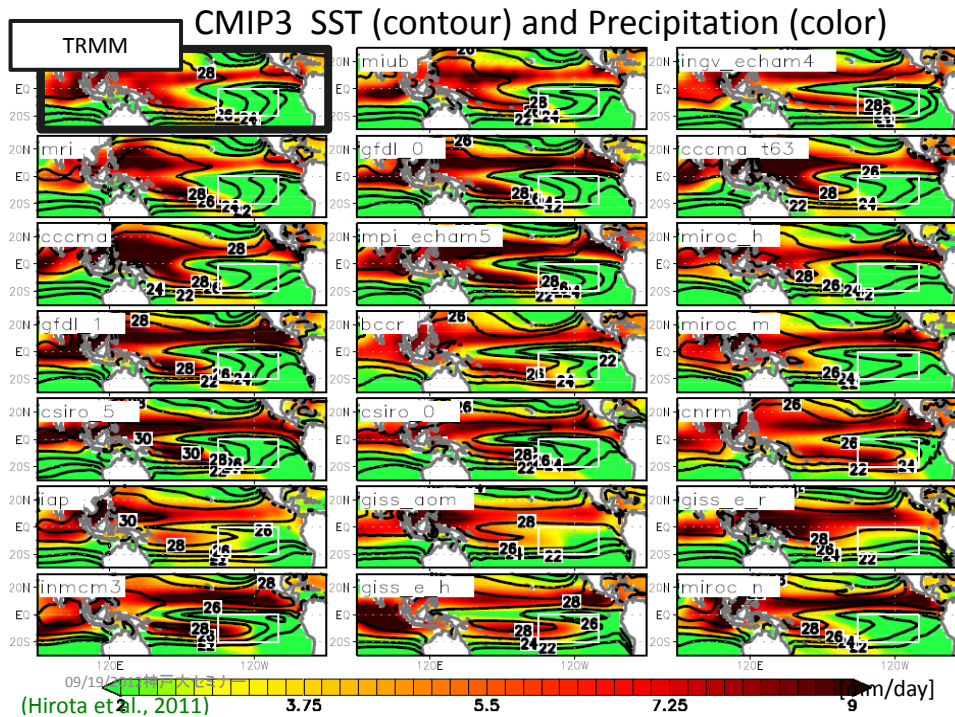
09/19/2012神戸大セミナー

熱帯海洋上の降雨分布とCMIP3, CMIP5モデル
のダブルITCZ問題

✓ 深い対流のSSTと環境場の湿度への感度

Precipitation distributions over the tropical oceans and the double ITCZ problem in CMIP3 and MIROC5 models are investigated, in terms of sensitivity of deep convection to SST and environmental humidity.

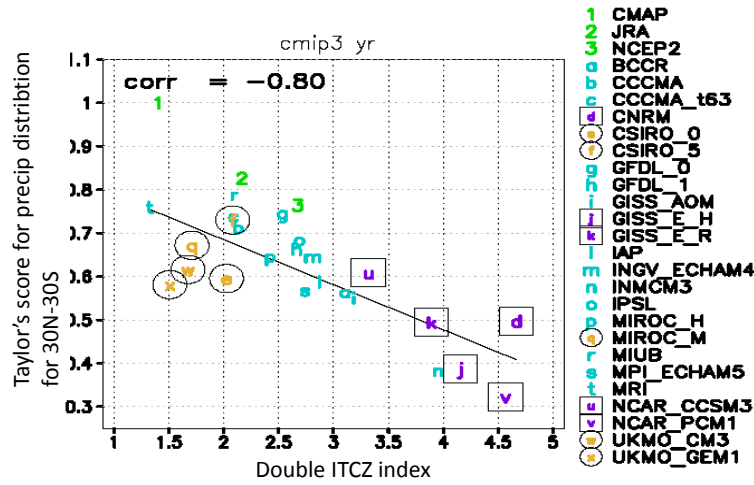
09/19/2012神戸大セミナー



Observation	TRMM PR 2A25
CMIP3	
BCCR	GISS_E_R
CCCMA*	IAP
CCCMA_t63*	INGV_ECHAM4
CNRM	INMCM3*
CSIRO_0	MIROC_H
CSIRO_5	MIROC_M
GFDL_0	MIUB*
GFDL_1	MPI_ECHAM5
GISS_AOM	MRI*
GISS_E_H	(*flux adjustment)
For CMIP5	MIROC5

Precipitation distributions in CMIP3 models and new MIROC5 are evaluated against the TRMM Precipitation Radar data

Double ITCZ ~ Taylor(2001)'s score for tropical precip.



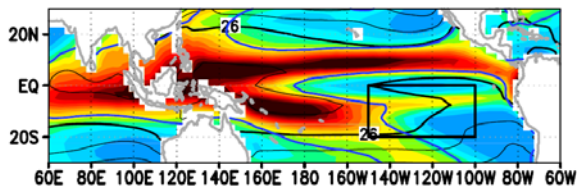
Among CMIP3 models, Taylor(2001)'s score for tropical (30N-30S) annual precipitation and the double ITCZ index have a significant negative correlation.

09/19/2012神戸大セミナー

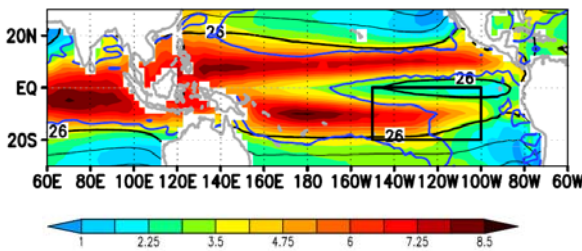
Modified from Hirota et al. 2011 JC

CMIP3 High and Low Performance Models in tropical precip. distribution(30N-30S 0-360E)

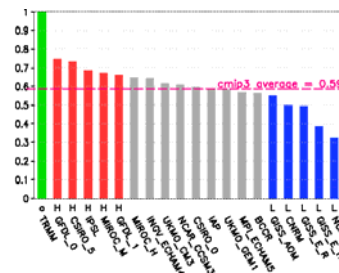
5 High Performance Models



5 Low Performance Models



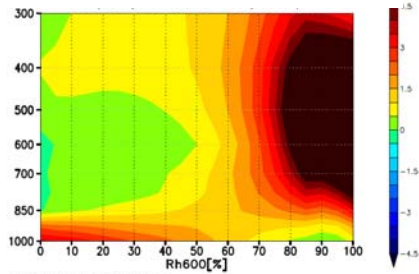
High performance models in terms of precipitation distribution also behave well with ITCZ structure, for CMIP3 models.



09/19/2012神戸大セミナー

Diabatic Heating (Q1) sorted with RH600hPa

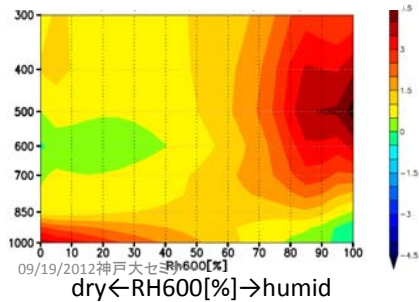
5 High Performance Models



CMIP3

Convection in high performance models is more sensitive to the mid-to-lower tropospheric relative humidity. So that deep convection is effectively suppressed when the RH600 is low. (Hirota et al., 2011)

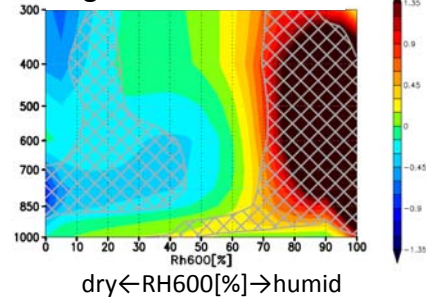
5 Low Performance Models



09/19/2012神戸大セミナー

dry ← RH600 [%] → humid

High PM – Low PM



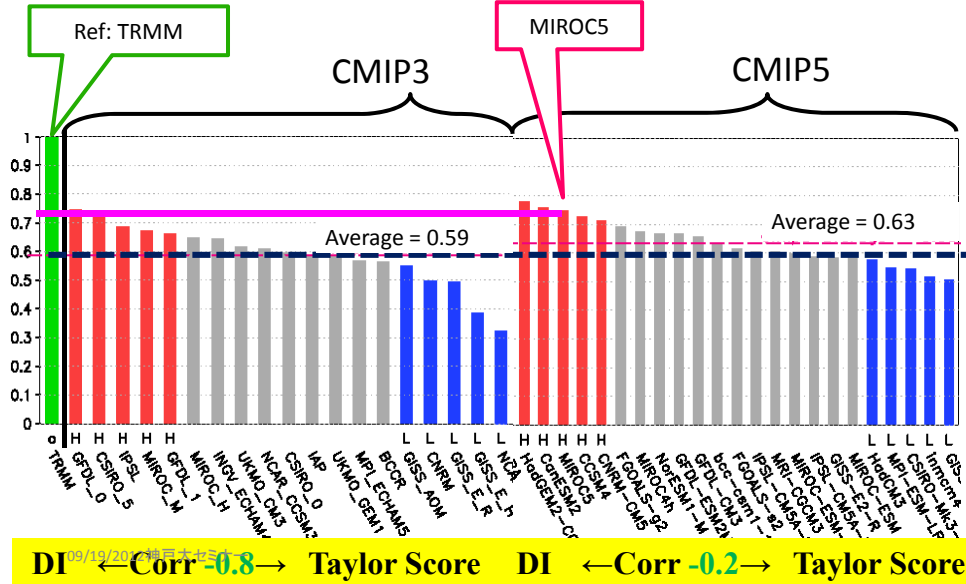
dry ← RH600 [%] → humid

CMIP5 CASE

09/19/2012神戸大セミナー

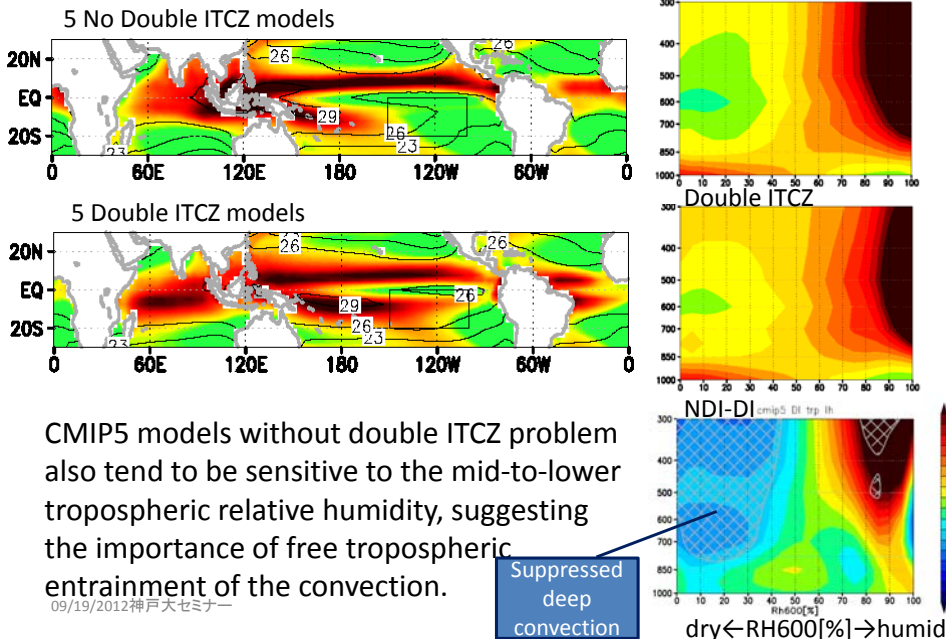
Taylor's score for tropical precip.: CMIP3 vs CMIP5

$$S \equiv \frac{(1 + R)^4}{4(SDR + 1/SDR)^2} \quad (\text{Taylor, 2001}) \quad (\text{Hirota et al., 2012})$$



CMIP5 for ITCZ distribution

(Hirota et al., 2012)



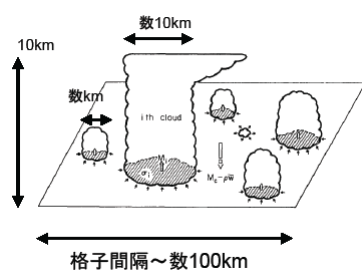
CMIP5 models without double ITCZ problem also tend to be sensitive to the mid-to-lower tropospheric relative humidity, suggesting the importance of free tropospheric entrainment of the convection.

09/19/2012神戸大セミナー

EFFECT OF ENTRAINMENTS

09/19/2012神戸大セミナー

A-S Cumulus parameterization



Spectral representation of
cumulus convection
Arakawa and Schubert (1974)

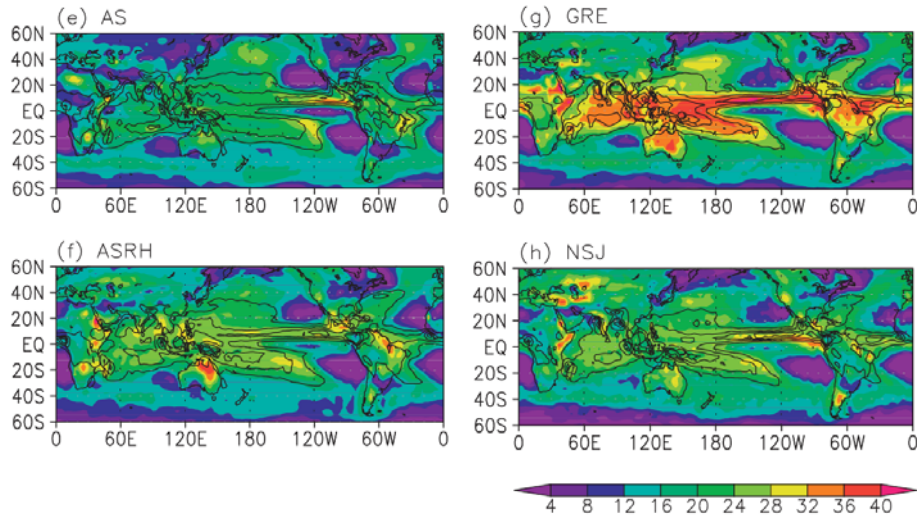
Treatment of entrainments

$$\frac{1}{M_c(z)} \frac{dM_c(z)}{dz} = \epsilon(z)$$

- Arakawa and Schubert (1974): $\epsilon(z) = \frac{2\alpha}{R}$
- Chikira and Sugiyama (2010): $\epsilon(z) = C_\epsilon \frac{aB(z)}{\hat{w}_c(z)^2}$

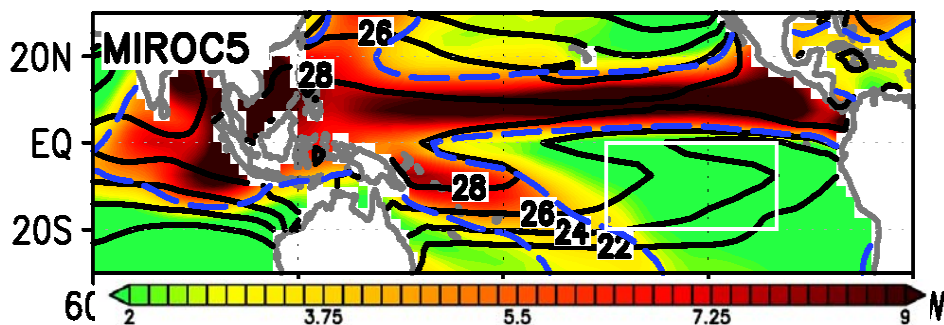
09/19/2012神戸大セミナー

Chikira 2010b

Fraction of detrainments at $\eta_{\text{eta}}=0.55$ to total

Cumulus congestus related detrainments increases with the modified GRE entrainment scheme

09/19/2012神戸大セミナー

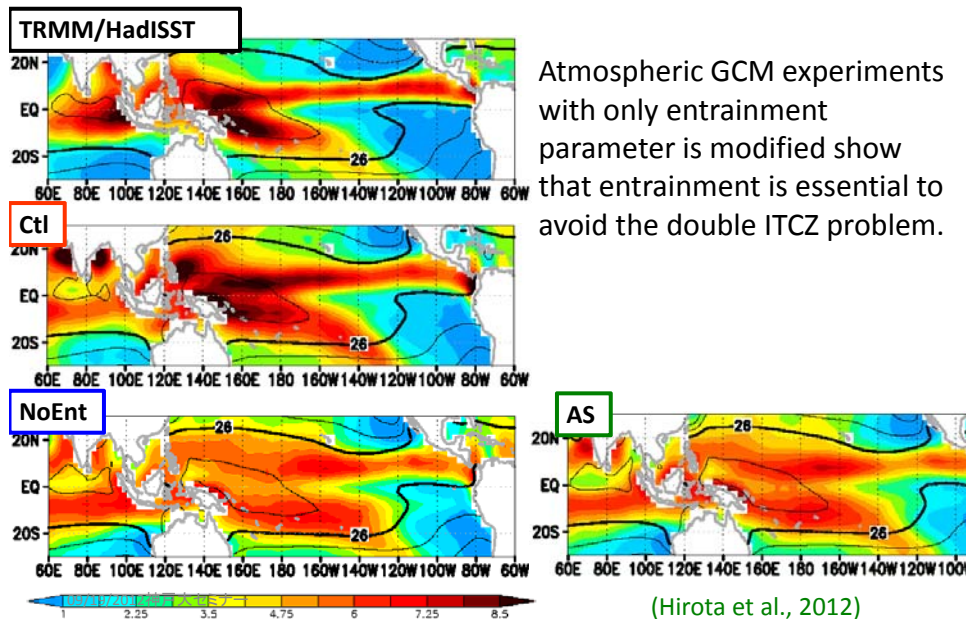
Precipitation, SST, and dp/dt_{500} 

MIROC5 with Chikira's implementation of modified GR01 state-dependent entrainment to AS parameterization, shows a good performance. Deep convection is largely suppressed with subsidence over moderately warm SST regions.

09/19/2012神戸大セミナー

(Hirota et al., 2011)

Precipitation Distributions in TRMM and MIROC-AGCM



Message

To avoid the double ITCZ problem in climate models, **a proper treatment of entrainment** of the tropospheric air in the cumulus parameterization is essential.

ただし、SSTバイアスの要因には、積雲のパラメタリゼーションに加えてもうひとつの要素があることが、CMIP5の解析から示唆されている。(解析中)

- Derbyshire, S. H. et al. 2004: Sensitivity of moist convection to environmental humidity. *Q. J. R. Meteorol. Soc.*, 130, 3055-3079.
- Kuang, Z., and C. S. Bretherton, 2006: A mass-flux scheme view of a high-resolution simulation of a transition from shallow to deep cumulus convection. *J. Atmos. Sci.*, 63, 1895-1909.
- Khairoutdinov, M. and D. Randall, 2006: High-resolution simulation of shallow-to-deep convection transition over land. *J. Atmos. Sci.* 63, 3421-3436.
- Del Genio, A. D., and J. Wu, 2010: The role of entrainment in the diurnal cycle of continental convection. *J. Clim.* 23, 2722-2738.

WHAT HAVE BEEN SHOWN FROM CRM STUDIES

09/19/2012神戸大セミナー

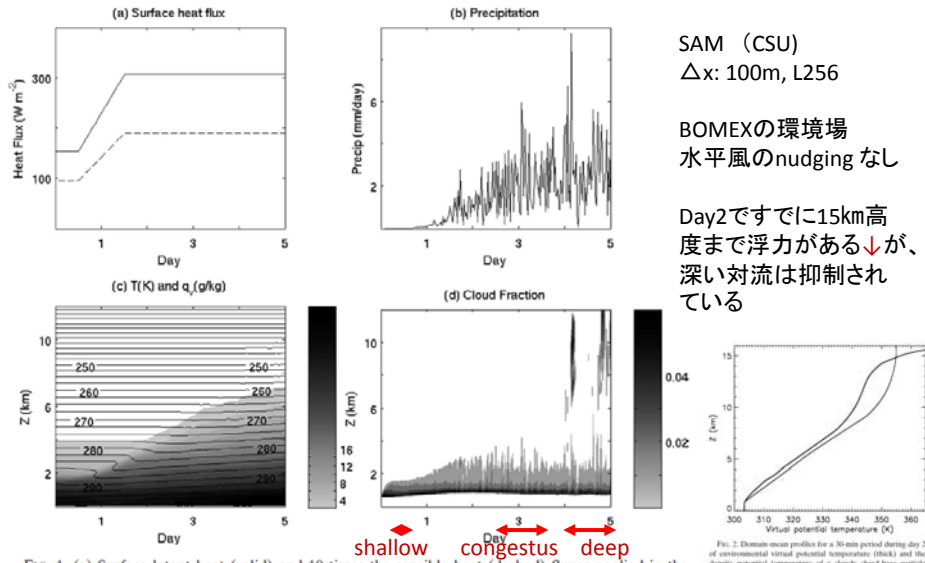
Khairoutdinov and Randall 2006



FIG. 2. Visualization of the simulated cloud field at 0130 in the afternoon as would be seen from the surface. Note that the clouds on the left are as high as 12 km.

09/19/2012神戸大セミナー

Kuang and Bretherton 2006



SAM (CSU)
 Δx : 100m, L256
 BOMEXの環境場
 水平風のnudgingなし
 Day2ですでに15km高度まで浮力がある↓が、深い対流は抑制されている

FIG. 1. (a) Surface latent heat (solid) and 10 times the sensible heat (dashed) fluxes applied in the experiment, and the evolution of domain-mean (b) precipitation, and profiles of (c) temperature (contours) and water vapor specific humidity (shading), and (d) cloud fraction.

FIG. 2. Domain-mean profiles for a 30 min period during day 2 of environmental virtual potential temperature (thick) and the density potential temperature of a cloudy cloud-base particle filled adiabatically without mixing (all condensates are retained in the parcel).

Kuang and Bretherton 2006

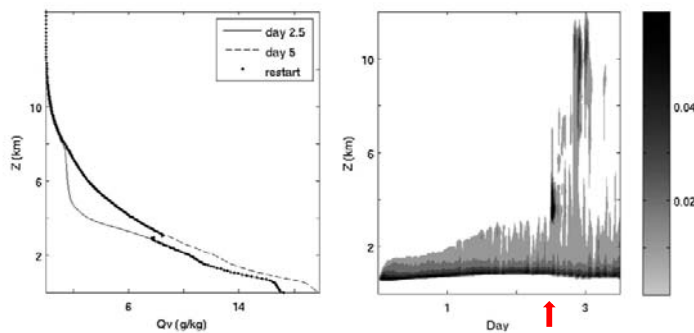


FIG. 3. (a) Domain-averaged q_v profile at the end of day 2.5 (solid) and day 5 (dashed) of the control run. The difference between the dotted line and the solid line was added to the new run, which restarted at the end of day 2.5 of the nominal run. (b) The evolution of cloud fraction profile in the restarted run. The first 2.5 days are the same as the nominal run shown in Fig. 1d.

Day2.5以降、 $z > 3\text{km}$ の比湿に下駄: day5の比湿を与える
 →即座にdeep convectionが発生

Kuang and Bretherton 2006

Cloudy mass flux
Shallow regime

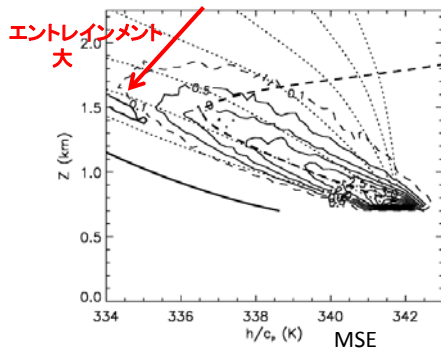


FIG. 9. The cloudy updraft/downdraft mass flux at each height binned by their MSE h (expressed as h/c_p in temperature units). The bin size is 0.18 K. The interval of the solid contours is $0.5 \text{ g m}^{-2} \text{ s}^{-1} \text{ bin}^{-1}$, the dashed contour is for $0.1 \text{ g m}^{-2} \text{ s}^{-1} \text{ bin}^{-1}$, and the thick solid contour is for $-0.1 \text{ g m}^{-2} \text{ s}^{-1} \text{ bin}^{-1}$, representing the downdrafts. The dotted lines are the MSEs predicted by entraining plume models with fractional entraining rates of (from right to left) 0.0625 km^{-1} , 0.125 km^{-1} , 0.25 km^{-1} , ..., 4 km^{-1} . The thick solid line to the far left is the domain mean MSE profile, and the thick dashed line is the domain mean saturation MSE profile.

deep regime

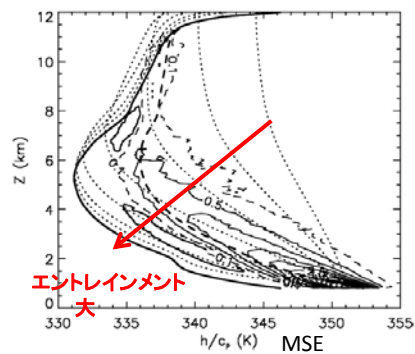


FIG. 11. Same as Fig. 9, except for the deep cumulus regime and for a bin size of 0.5 K in h/c_p .

Shallow cloudsの方がエントレインメント率が高い。ただ、Deep cloudsも 0.125 km^{-1} 線を下回らない。Size dependencyの示唆。

Khairoutdinov and Randall 2006

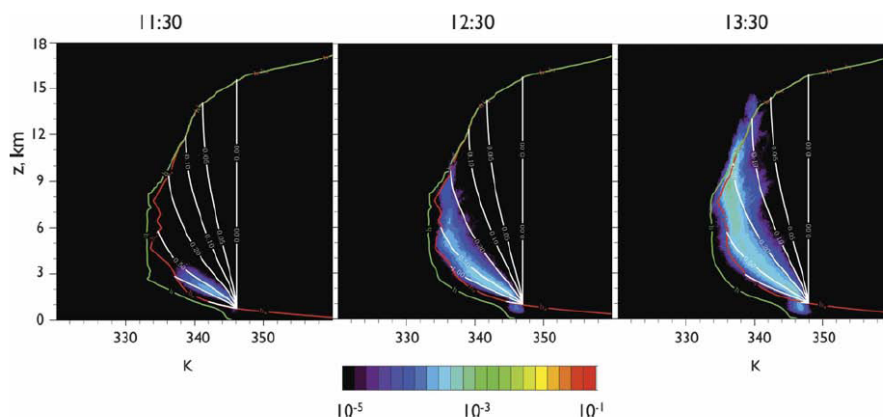


FIG. 12. As in Fig. 11 except for the updraft cores defined by the vertical velocity being in excess of 5 m s^{-1} .

Khairoutdinov and Randall 2006

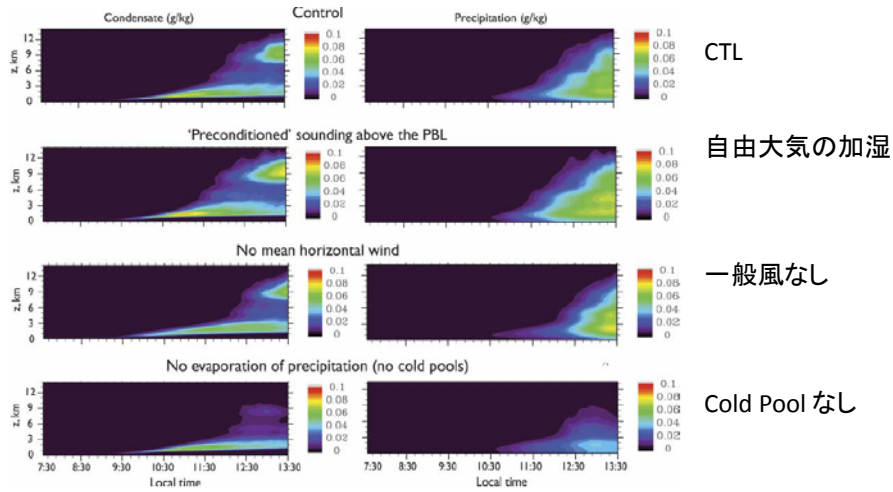


FIG. 15. Evolution of mean vertical profiles of (left) nonprecipitating cloud condensate and (right) precipitating water for the (top) control run and (bottom) three sensitivity runs (see text for details).

09/19 気象学
 感度実験: この実験では、中層はすでに十分湿っていたので、湿度の上乗せにはさほど感度がないが、効果は見える。Cold Poolは大きなBoundary Layer thermalを作ることを通じて、entrainmentの小さい対流を可能にすると解釈。

Del Genio and J. Wu 2010

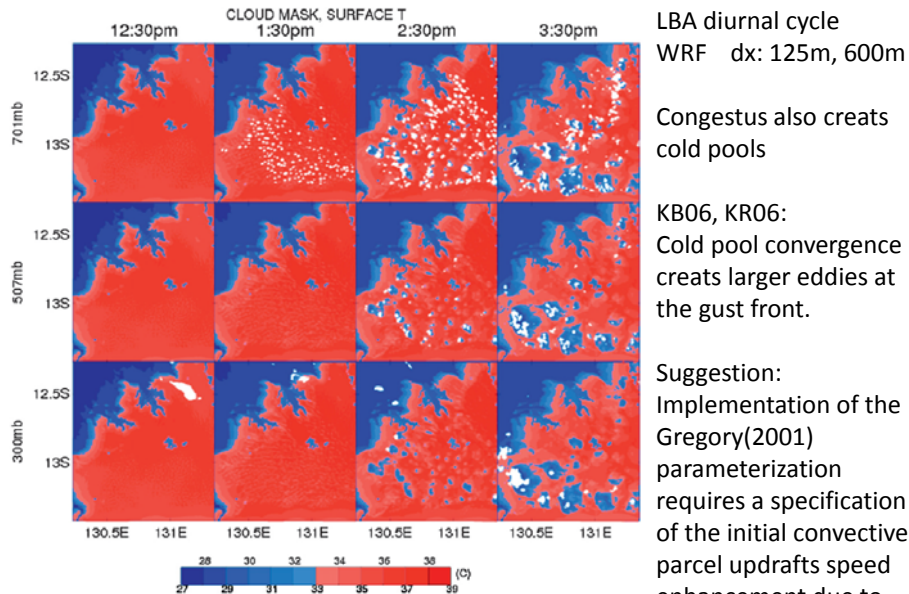


FIG. 4. Near-surface temperature, with cloud mask overlain in white, at (top) 701, (middle) 507, and (bottom) 300 mb at different times of day in the CONTROL simulation.

Congestus also creates cold pools

KB06, KR06:
 Cold pool convergence creates larger eddies at the gust front.

Suggestion:
 Implementation of the Gregory(2001) parameterization requires a specification of the initial convective parcel updrafts speed enhancement due to downdraft cold pool convergence.

CRM studiesから

- 中層(>3km)の湿度が深い対流にもたらす効果を確認
- エントレインメントのサイズ依存性: 浅い雲の方が深い雲より大きい。雲のサイズが大きい方がentrainment小さい。
- ただし、深い(大きい)雲でもentrainmentが0.1を下回らない。
- Congestus(雄大積雲:水雲)でも、cold poolが形成される。
- Cold poolがより大きいplumeの生成を通じて深い対流をトリガーする効果の重要性が指摘された

09/19/2012神戸大セミナー

まとめ

- From long-term TRMM data, the effect of the large-scale subsidence was observationally indicated. It suppresses the deep convection through drying the mid-level troposphere, thus generating cumulus congestus regime of precipitation.
- The “double ITCZ problem” in climate models is closely linked to the sensitivity of the cumulus parameterization to the tropospheric humidity.
- Above results are in concert with MIROC5 with the state-dependent entrainment rate (Chikira and Sugiyama 2010)
- Significant role of cold pools for triggering the deep convection has been suggested from CRM studies.

09/19/2012神戸大セミナー